A Unified Framework for Vehicle Rerouting and Traffic Light Control to Reduce Traffic Congestion

Zhiguang Cao, Siwei Jiang, Jie Zhang, and Hongliang Guo

***Abstract*— As the number of vehicles grows rapidly each year, more and more traffic congestion occurs, becoming a big issue for civil engineers in almost all metropolitan cities. In this paper, we propose a novel pheromone-based traffic management framework for reducing traffic congestion, which unifies the strategies of both dynamic vehicle rerouting and traffic light control. Specifically, each vehicle, represented as an agent, deposits digital pheromones over its route, while roadside infrastructure agents collect the pheromones and fuse them to evaluate real-time traffic conditions as well as to predict expected road congestion levels in near future. Once road congestion is predicted, a proactive vehicle rerouting strategy based on global distance and local pheromone is employed to assign alternative routes to selected vehicles before they enter congested roads. In the meanwhile, traffic light control agents take online strategies to further alleviate traffic congestion levels. We propose and evaluate two traffic light control strategies, depending on whether or not to consider downstream traffic conditions. The unified pheromone-based traffic management framework is compared with seven other approaches in simulation environments. Experimental results show that the proposed framework outperforms other approaches in terms of traffic congestion levels and several other transportation metrics, such as air pollution and fuel consumption. Moreover, experiments over various compliance and penetration rates show the robustness of the proposed framework.**

***Index Terms*— Agent-based traffic management, pheromone, proactive vehicle rerouting, online traffic light control.**

I. Introduction

With increasing traffic volumes and limited road capacities, *traffic congestion* has become a big issue for civil engineers in almost all modern metropolitan cities like London, New York and Singapore [1]. Traffic congestion can lead to a variety of social, economical and environmental problems. First, drivers, when stuck in traffic congestion, are facing a higher risk of arriving late at their destination, causing great levels of stress. The stress may further transform into impatience, carelessness, and hence increase the occurrence rate of traffic accidents and other social problems like road rage [2]. Second, economic cost from traffic congestion is also enormous. According to the urban mobility report [3] by the Texas Transportation Institute (TTI), the average delay per commuter per year is around 34 hours, so that the total cost of congestion in the USA is estimated to be roughly $100 billion annually, or $750 per commuter. In addition, 1.9 billion gallons of fuel are wasted due to road congestion. Last but not the least, traffic congestion also has a negative impact on the environment. The longer the vehicles remain stuck on the road, the more fuel they consume, resulting in higher CO_2 pollution and posing a higher health risk to inhabitants.

To address the traffic congestion problem, traffic engineers tend to seize the opportunity of the recent development of data sensing and communication technologies, and develop intelligent transportation systems (ITSs) that employ apply artificial intelligence techniques over collected and/or communicated traffic information to direct traffic flow. Therefore, ITSs have become more and more popular [4]–[6]. In general, ITS solutions to alleviate traffic congestion can be divided into two categories [1], [7]: 1) to reroute some of the vehicles away from the 'to-be-congested' areas; 2) to explore traffic light control policies to more efficiently make use of road resources. Detailed literature review will be provided in Section II.

In this paper, we propose a novel multiagent pheromone-based traffic management framework to reduce traffic congestion. It bridges vehicle rerouting and traffic light control by bringing about the notion of digital "pheromone." Specifically, each vehicle agent deposits two types of pheromones (i.e., traffic pheromone and intention pheromone representing the current and future traffic densities, respectively) along its route. Roadside infrastructure agents combine the pheromones using a fusion or regression model, to forecast the short-term traffic conditions without resorting to the central ITS server, achieving the distributed property. Once road congestion is predicted, our framework adopts a proactive vehicle rerouting strategy, which first selects vehicles that need rerouting, and then assigns alternative routes to them before they enter congested roads. In the meanwhile, two online traffic light

Manuscript received August 21, 2015; revised February 3, 2016, April 26, 2016, and July 13, 2016; accepted September 17, 2016. Date of publication October 12, 2016; date of current version June 26, 2017. The work of J. Zhang was supported by the MOE AcRF Tier 1 Funding under Grant M4011261.020. The Associate Editor for this paper was B. F. Ciuffo. *(Corresponding author: Hongliang Guo.)*

Z. Cao is with the School of Computer Science and Engineering, Nanyang Technological University, Singapore 639798, and also with the Interdisciplinary Graduate School, Nanyang Technological University, Singapore 639798 (e-mail: caoz0005@e.ntu.edu.sg).

S. Jiang is with the Singapore Institute of Manufacturing Technology, Singapore 638075 (e-mail: jiangsw@simtech.a-star.edu.sg).

J. Zhang is with the School of Computer Science and Engineering, Nanyang Technological University, Singapore (e-mail: zhangj@ntu.edu.sg).

H. Guo is with the School of Automation Engineering, University of Electronic Science and Technology of China, Chengdu 611731, China, (e-mail: guohl1983@uestc.edu.cn).

Color versions of one or more of the figures in this paper are available online at http://ieeexplore.ieee.org.

Digital Object Identifier 10.1109/TITS.2016.2613997

control strategies, i.e., TLC-NCDT (traffic light control not considering downstream traffic) and TLC-CDT (traffic light control considering downstream traffic), are designed to assign suitable time duration of traffic lights. We would like to highlight that, the proposed pheromone-based traffic management framework is a decentralized approach where vehicles exchange traffic information with the local and distributed roadside infrastructures.

The unified traffic management framework is tested on the platform of simulation of urban mobility (SUMO) [8]. Extensive experimental results show that our framework significantly alleviates traffic congestion (hence saves drivers' travel time), and reduces air pollution and fuel consumption. Moreover, simulation results show that our framework is robust to different levels of compliance and penetration rates.

The rest of this paper is organized as follows. Section II lays down related work and the contributions of our work. Section III illustrates the overall structure of our traffic management framework. Section IV describes the pheromone-based traffic congestion forecasting model, followed by the pheromone-based vehicle rerouting strategy in Section V. The two different pheromone-based traffic light control strategies are presented in Section VI. Section VII presents experimental settings, comparative results and corresponding analysis. Section VIII proposes an improvement to our unified framework, which is also justified through experiments. Section IX discusses several issues and possible solutions when implementing our pheromone based framework in practice. The paper ends with conclusions and potential future works in Section X.

II. Related Work

A transportation system can be formulated as an open, large scale, distributed and dynamic multiagent system, in which vehicles, roadside infrastructures and traffic lights can be represented as agents. A typical scenario of a multiagent transportation system is described as follows: vehicle agents inquire traffic information (e.g., road coverage rate, mean speed) from roadside infrastructure agents (e.g., loop detectors, video cameras) for routes with smaller travel cost [9]; on the other hand, all vehicles must obey instructions from traffic light control agents to pass or stop at road intersections.

In this section, we survey the state-of-the-art approaches from multi-agent perspective to alleviate traffic congestion. Recently, multiagent techniques [10]–[19] have gained popularity in intelligent transportation systems (ITS) for the purpose of alleviating traffic congestion. Based on various applications, they can be generally divided into two categories, namely vehicle rerouting [10]–[17], [20] and traffic light control [18], [19], [21], [22].

Agent-based vehicle rerouting approaches intend to offer alternative routes to some of the vehicles so that the overall traffic congestion level is alleviated. One of the challenges in vehicle rerouting is the requirement of real time reaction (drivers cannot wait too long for a rerouted path). To quickly respond to route inquires, Wu *et al.* [20] propose to precompute shortest paths among transit nodes or landmarks (referred to as important nodes) on a single snapshot of traffic map. When a driver asks for an origin-destination service from the ITS server, it only needs to calculate partial paths, e.g., the path from the origin/destination nodes to the important nodes.

Another challenge is to make use of real time traffic information. Commercial systems developed by companies (e.g., Google, Mircrosoft and TomTom) make use of roadside infrastructures to collect dynamic traffic information and provide traffic-aware shortest routes. Although these systems are able to predict long-term traffic congestion and its duration using advanced data mining techniques, they are often used as reactive solutions that remain unable to prevent congestion. In addition, these system may cause "route flapping" [14] where congestion switches from one road to another road when a significant number of vehicles are following the same route guidance. So, some vehicle rerouting approaches [10]–[12], [14]–[17], [23], [24] proactively direct vehicle agents to avoid traffic congestion. For instance, Ando *et al.* [10], [12] introduce the "pheromone" concept from bio-inspired techniques [18] to forecast short-term traffic congestion. Each vehicle deposits three types of pheromones (i.e., basic traffic pheromone, braking pheromone, distance pheromone) on its route, which represent the traffic information of speed, halting vehicles and distance between two vehicles. Kurihara [11] defines the digital pheromone as two kinds of traffic information, such as the upstream flow of traffic density and the downstream flow of traffic congestion. Then, the distributed roadside infrastructures in [10]–[12] combine the multiple flavors of digital pheromones to predict short-term traffic conditions. On the other hand, Pan *et al.* [14] count the number of vehicles on different roads to estimate the current traffic conditions. Once congested roads are predicted, they recursively apply the k-shortest path on vehicles to find alternative routes. However, these approaches [10]–[12], [14] forecast traffic congestion based only on historical data while ignoring another important traffic information, i.e., drivers' route intention of changing directions in the near future [15]–[17]. For instance, Dresner and Stone [15] and Vasirani and Ossowski [16] design the reservation-based method to manage traffic flows according to drivers' route intentions. Yamashita *et al.* [17] adopt the similar idea that all vehicles report the route information to the central ITS server including current position, destination and route to destination.

Besides vehicle rerouting, traffic light control [18], [19] also serves as an effective approach to manage traffic flows. Traditional traffic light control in ITSs often adopts fixed color phases and predefined time duration, which is usually inefficient for dynamic traffic conditions. Therefore, some researchers aim to alleviate traffic congestion levels through adapting traffic light schedules. For instance, Wiering *et al.* [19] adopt reinforcement learning to minimize the overall waiting time of vehicles. However, this approach is not suitable for large-scale traffic scenarios since it needs to store the global information of all traffic lights. Park *et al.* [25] develop a generic algorithm for traffic signal timing, where three optimization strategies were tested: throughput maximization, delay minimization, and modified

delay minimization with a penalty function. The experiments show that the delay minimization strategy is recommended since it is applicable to both under-saturated and over-saturated traffic conditions. José *et al.* [18] utilize the genetic algorithm to find the optimal combination of traffic lights. In particular, the evolutionary optimizer is an offline algorithm using the trial-and-error procedure. It is only designed for simulations, because vehicles' movement in realistic transportation systems is irrevocable. Additionally, based on the concept of retrospective approximation (RA), Li *et al.* [21] develop an optimal design of the maximum green setting for traffic lights with the multi-detector green extension system. They also designed a variant of Markov monotonic search algorithm which accommodates the requirements of the RA framework. The algorithm presents promising ability to reduce delay and increase safety in the simulator of VISSIM. Then, Li *et al.* [22] also present a new approach of traffic light control to minimize the vehicles fuel consumptions on arterials. They adopt generated total fuel consumption as the objective function for optimizing signal timings, which is solved by the Lagrangian Relaxation framework. To mitigate the negative impacts of spillbacks, de Lamberterie *et al.* [26] present a traffic signal control for global management of long queues along signalized road links. In that method, they implement a real-time partitioning of the road links to detect critical group of consecutive links with over-saturated traffic conditions. Experimentation on a real-world network demonstrates its advantage of reducing the delay time on the road links even with a high level of traffic in cross-streets. Considering spill-overs control, Jang *et al.* [27] propose a method of queue growth equalization (QGE), for optimizing traffic signal timing in over-saturated traffic situation, which adopts the degree of QGE as a new measure of effectiveness and minimizes the degree of QGE to balance queue growth rates over the network. Simulation results show that the QGE based method is able to successfully distributed queues over the upstream links, which otherwise would have spilled over into the network.

Vehicle rerouting and traffic light control can individually help to alleviate traffic congestion, and it is desirable to combine them together as a traffic management framework. For instance, Yang and Yagar [28] propose to formulate congestion alleviation as a bi-level programming problem. The lower-level problem predicts how drivers will react to any given signal control pattern. The upper-level problem is to determine signal splits to optimize a system objective function of drivers' route choice behavior in response to signal split. However, this framework is derived based on the assumption of equilibrium flows, which is not realistic because traffic is always much more dynamic and complex. Besides, Li *et al.* [29] address the problem of simultaneous route guidance and traffic signal optimization problem (RGTSO) based on a space-phase-time hypernetwork. In this framework, each vehicle is guided on a path and the traffic signals servicing those vehicles are set to minimize their travel time, which is finally decoupled and solved by the Lagrangian Relaxation optimization framework. In addition, Bazzan *et al.* [1] propose an evolutionary algorithm to try out a large number of candidate solutions (i.e., diversified routes and traffic signals), and find solution with the best fitness based on simulation. However, this approach does not optimize the two components in a simultaneous manner under a unified framework.

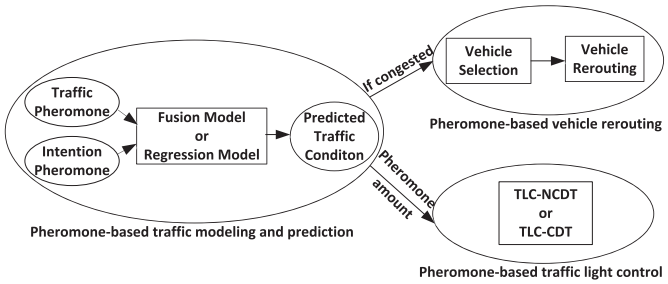

Fig. 1. Pheromone-based traffic management framework.

In view of this, we propose a multiagent traffic management framework in this paper, which unifies vehicle rerouting and traffic light control by the notion of digital "pheromone," with the novelty and contributions summarized as follows:

- we are the first to use a pheromone-based method to combine vehicle rerouting and traffic light control, to alleviate traffic congestion;
- we propose to utilize the digital pheromone involving drivers' route intention in predicting the short-term traffic conditions;
- we propose a proactive pheromone-based vehicle rerouting algorithm to direct vehicles away before they enter congested roads;
- the proposed traffic management framework is a decentralized approach, which is applicable to large scale road networks.

III. The Unified Pheromone-Based Traffic Management Framework

As shown in Fig. 1, our framework is composed of three components, namely, pheromone-based traffic modeling and prediction, pheromone-based vehicle rerouting strategy, and pheromone-based traffic light control. The motivation is to unify vehicle rerouting and traffic light control by bringing about the notion of digital "pheromone."

To be more specific, in our framework, each vehicle agent deposits traffic pheromone and intention pheromone along its route, which respectively represents current and future traffic densities. Roadside infrastructure agents, to achieve the distributed property, locally combine the pheromones using a fusion or regression model, to forecast the short-term traffic conditions without resorting to the central ITS server. Once road congestion is predicted, our framework adopts a proactive vehicle rerouting strategy, which first selects vehicles that need rerouting, and then assigns alternative routes to them before they enter congested roads. In addition, based on pheromone amount of the concerned road links, an online traffic light control strategy, i.e., TLC-NCDT (traffic light control not considering downstream traffic) or TLC-CDT (traffic light control considering downstream traffic), is designed to assign suitable time duration for traffic lights.

In the following three sections, we will lay down the unified pheromone-based traffic management framework. And the contents of the three components are displayed in Sections IV, V and VI respectively.

IV. Pheromone-Based Traffic Modeling and Prediction

Before performing agent-based vehicle rerouting or traffic light control, we have to build a model to evaluate the current traffic condition and predict short-term traffic congestion levels. This section elaborates the pheromone-based traffic modeling and prediction, where two types of pheromones (i.e., traffic pheromone and intention pheromone) are considered.

A. Traffic Pheromone and Intention Pheromone

In nature, the term "pheromone" refers to communication chemical that is mutually understood by the individuals of the same species [10], [12]. For instance, ants use a trail pheromone (intensity of flavors) to guide others on routes for food foraging. Inspired by this phenomenon, we define two types of digital pheromones, i.e., traffic pheromone and intention pheromone, to represent the current and future road conditions, respectively.

The *traffic pheromone* is defined as:

$$\tau_1(p,t) = \frac{N(p,t) \times L_{\text{veh}}}{L_p \times \text{lanes}(p)}, \tag{1}$$

where $N(p,t)$ with the unit of amount is the vehicle count on road p in time $(t-1,t]$, L_{veh} with the unit of meter is the mean length of vehicles,[1] L_p with the unit of meter is the length of road p, and lanes(p) with the unit of amount is the number of lanes on p. The traffic pheromone without an explicit unit, is used to estimate the current road coverage rate. In a traffic map, a large road coverage rate means that many vehicles are moving on a road, and implies that traffic congestion may occur in the near future.

When a road congestion is detected, vehicles on this road have to find new routes. However, this reactive process may be too late since traffic jam may have already been formed. It is thus important to forecast the short-term traffic congestion before a driver decides which road to proceed (we note that in our case it is useless to forecast long term traffic congestion, e.g., 1 day). In this case, a proactive action is beneficial for distributing traffics onto different roads before traffic congestion really occurs.

To predict the short-term traffic conditions, we absorb another important traffic information, i.e., drivers' route intention [30], [31]. This makes our digital pheromone different from the exiting definitions [10]–[12], [32]. Suppose that each vehicle reports its route to a local roadside infrastructure (e.g., using smart phones). The *intention pheromone* is used to estimate the near future road coverage rate, and defined as:

$$\tau_2(p,t+1) = \frac{[I(p,t+1) - O(p,t+1)] \times L_{\text{veh}}}{L_p \times \text{lanes}(p)}, \tag{2}$$

[1] L_{veh} is the sum of the vehicle length and the gap between two vehicles.

where $I(p,t+1)$ and $O(p,t+1)$ with the unit of amount are the the numbers of incoming and outgoing vehicles on road p in time $(t,t+1]$, respectively. Note that these two terms describe the near future road conditions (i.e., the time of $(t,t+1]$). Both $I(p,t+1)$ and $O(p,t+1)$ take the similar formulation. For instance, we define the incoming traffic volume $I(p,t+1)$ as:

$$I(p,t+1) = \sum_{p' \in P_{\text{nei}}} f(p') T_g(p') \times \rho, \tag{3}$$

where $I(p,t+1)$ is the number of vehicles that will move from the neighboring roads $p' \in P_{\text{nei}}$ to road p in time $(t,t+1]$; $f(p') = V_f(p')N(p',t)/L_{p'}$, is the estimated flow rate wherein $V_f(p')$ is the free speed of road p'; $T_g(p')$ is the time duration of the green traffic light on road p'; and ρ is the proportion of vehicles that have the intention of moving from road p' to road p and are able to pass the stop-line during latest green color. Particularly, we first count vehicles having intentions of moving from p' to p, and among them, we further count vehicles that can pass the stop-line within latest green color duration, which can be approximately achieved based on current location and speed of each involved vehicle. Thus, ρ can be easily calculated.

B. Traffic Prediction by Pheromone

Traffic condition prediction is an attractive topic in transportation management, and there are still many challenging problems in short-term traffic forecasting, one of which is how to fuse the traffic data [33]. Generally, there are two categories to fuse the data in short-term traffic prediction: parametric approach (e.g., linear regression and time series) and non-parametric approach (e.g., artificial neural network) [34]. In our framework, to fuse the above two types of digital pheromones, we design two different approaches, i.e, a simple fusion model (a linear model) and a support vector regression model (SVR, an artificial neural network model).

1) Pheromone Fusion Model: The simple fusion model defines an evaporation rate to update digital pheromone. In particular, the natural process of pheromone update includes evaporation and propagation. Evaporation means that the old pheromone will disappear as time passes. Propagation implies that pheromone spreads to the surrounding environments. From Eq. (2), the intention pheromone $\tau_2(p,t+1)$ can be considered as a type of propagation, which defines the incoming and outgoing vehicles in the neighboring roads. In our model, the evaporation rate is defined in Eq. (4).

$$e(p,t) = \frac{\bar{V}(p,t)}{V_f(p)} \times \frac{1}{1 + |\text{Halts}(p,t)|}, \tag{4}$$

where $\bar{V}(p,t)$ is the mean speed of vehicles on road p in time $(t-1,t]$ and $|\text{Halts}(p,t)|$ is the number of halting vehicles that have stopped due to traffic congestion, traffic lights and so on, on road p in time $(t-1,t]$.

Then, the roadside infrastructures collect the two types of digital pheromones and fuse them according to Eq. (5).

$$\tau(p,t+1) = (1-e(p,t)) \times \tau_1(p,t) + e(p,t) \times \tau_2(p,t+1). \tag{5}$$

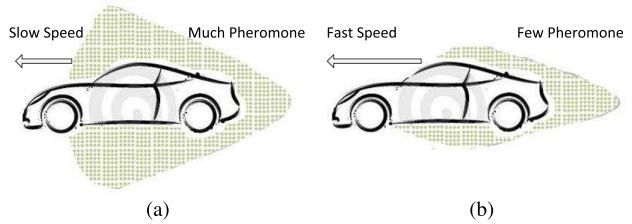

Fig. 2. Digital pheromone with different speed. (a) Many pheromones. (b) Few pheromones.

Take Fig. 2 as an example to explain Eqs. (4)-(5): the vehicle with slow speed will deposit much pheromone on the road in Fig. 2(a); on the contrary, the fast speed vehicle deposits few pheromone in Fig. 2(b). If the mean speed $\bar{V}(p,t)$ is large enough to reach the free speed $V_f(p)$, and $\frac{\bar{V}(p,t)}{V_f(p)}$ in Eq. (4) is equal to 1, then no traffic pheromone $\tau_1(p,t)$ will be deposited, as calculated through Eq. (5). On the other hand, the old pheromone will remain as the number of halting vehicles increases. Thus, the evaporation rate in Eq. (4) involves $\frac{1}{1+|\text{Halts}(p,t)|}$.

2) Pheromone Regression Model: Although the pheromone fusion model as described in the previous subsection is straightforward and easy to implement, in some cases, we still need to improve the prediction accuracy. Thus, we adopt one of the famous machine learning techniques (ϵ-SVR in LIBSVM [35]) as another model to combine the above two pheromones. In particular, the input training instances are $\{(x_1, z_1), \ldots, (x_t, z_t)\}$, where

$$x_t = (\tau_1(p, t-1), \tau_2(p,t)), \tag{6}$$

and

$$z_t = \tau(p,t) = \tau_1(p,t). \tag{7}$$

which are the feature vectors and target output, respectively. After getting the input pheromone information in time $(t-1, t]$ as $x = (\tau_1(p,t), \tau_2(p, t+1))$, the digital pheromone is forecasted as:

$$\tau(p, t+1) = z_{t+1} = \sum_{i=1}^{t}(-\alpha + \alpha^*)K(x_i, x) + b, \tag{8}$$

where α, α^*, b are estimated parameters by solving ϵ-SVR, and $K(\cdot)$ is RBF kernel and training set includes $t = 60$ instances.

C. Regulating the Prediction Steps

In Section IV-B, we can predict traffic condition one step away, and sometimes, prediction for a longer time is also needed. To achieve this, there are usually two feasible solutions. The first one is to directly enlarge the step size, e.g., to predict the traffic condition three minutes later, one can consider three minutes as one step, and then make prediction for one step away. Contrarily, the second solution is to predict the traffic condition more steps away while keeping a smaller step size, e.g., one can predict the traffic condition three steps away, with one minute as step size [36]. Generally, for short-term prediction, the second solution is superior to the first one due to the fine granularity [32], [37], [38].

Taking above concerns into account, in the fusion model, the regulation of prediction steps can be achieved by using the evaporation rate in Eq. (4) and Eq. (5), expressed as:

$$e(p,t,m) = \begin{cases} \beta_1, & \text{if } v(p,t,0) > m \cdot \nabla v_p \\ 1, & \text{if } -m \cdot \nabla v_p < v(p,t,0) \leq m \cdot \nabla v_p \\ \beta_2, & \text{if } v(p,t,0) \leq -m \cdot \nabla v_p \end{cases} \tag{9}$$

where $e(p,t,m)$ means the evaporation rate is m time steps away with respect to the current time t, $\beta_1 = 1.1$, $\beta_2 = 0.9$, and ∇v_p is the average change of the speed on road p, which can be learned from historical traffic data [36].

Similarly, in the regression model, we adapt the z_t in the training instance as $z_{t,m}$, which can be expressed as:

$$z_{t,m} = \tau(p,t,m) = \tau_1(p,t,m). \tag{10}$$

Then we take the training instance $(x_t, z_{t,m})$ into Eq. (8) to train the regression model.

V. Pheromone-Based Vehicle Rerouting

Once congestion is predicted for a road link, we first propose a scheme to select vehicles which need rerouting, then we develop a rerouting strategy to distribute them based on global distance and local pheromone.

A. Selection of Rerouting Vehicles

On one hand, once congestion is predicted for a road link, there is a potential risk of undesirable delay for those vehicles intending to travel on it. Therefore, it is important for them to avoid the congestion by rerouting. On the other hand, it is obvious that rerouting is not necessary for those vehicles far away from the congested road link. We use a meta parameter l (level) [14] to determine how far from congested roads the vehicles should be selected for rerouting. We only reroute the vehicles that are up to l-hop upstream of the concerned road link. The parameter l needs to be properly determined, in order to efficiently reduce the impact of congestion while not cause unnecessary rerouting of vehicles [39]. We would like to point out that, to select vehicles for rerouting, we may need to collect intentions of vehicles that are two or more road links away. While in Eq. (2), we only collect intentions of vehicles that are one road link away, to compute the intention pheromone.

However, l is not the only criterion for vehicle selection. As shown in Fig. 3, we assume that congestion is predicted on road link p_c, and road links p_1-p_8 are all within distance of l (i.e., $l = 2$) with respect to p_c, and the distance for road link p_9 is 3. But we notice that vehicles v_1, v_2, v_7 and v_8 originally do not intend to travel on p_c, and rerouting them will trigger unnecessary cost. Therefore, we combine the distance (l) and the vehicle intention as the criterion to select vehicles for rerouting. Here, we wish to note that a roadside infrastructure agent only locally collects the driving intention of vehicles according to l.

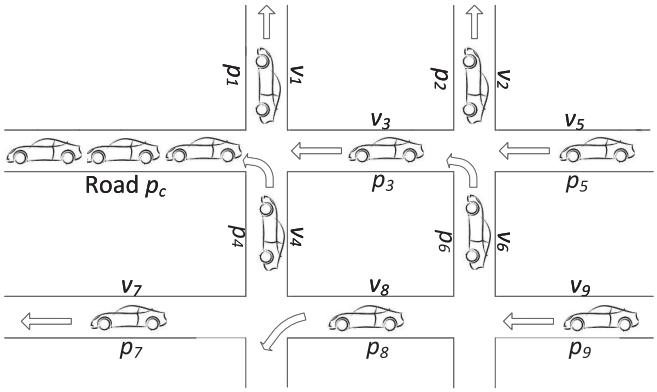

Fig. 3. Illustration of distance parameter l and intention of vehicles.

B. Rerouting Strategy

In an ideal rerouting strategy, global dynamic traffic information is desirable for avoiding congestion. However, in that case, it always falls into a centralized method [17], [31], which might become prohibitively expensive as the road network size and the number of involved vehicles scale up. We propose an decentralized vehicle rerouting strategy by combining the global distance information and local dynamic pheromone. The global distance information on a map is static and readily available on any in-vehicle system, and the local dynamic pheromone information can be collected from roadside units.

Intuitively, we can simply let rerouting vehicles switch to the second best path, once congestion is predicted to happen on the original best path. However, in this case, another congestion in a new place is likely to happen [40]. Therefore, it is desirable to distribute them to different paths and in the meanwhile not result in much unnecessary detour.

To this end, our rerouting strategy first computes k-shortest paths using the global distance for vehicles which needs rerouting [41]. Then it randomly chooses one path with certain probability, which is computed based on the sum of pheromone amount over the l downstream road links of each k-shortest path. Specifically, the probability for vehicle v_i to choose path j is expressed as:

$$Pb_j^i = \frac{e^{-\lambda \cdot \tau_j^l}}{\sum_{j=1}^{k} e^{-\lambda \cdot \tau_j^l}}, \tag{11}$$

where λ is a weight parameter, and τ_j^l is the pheromone sum of the current first l road links on the j-th shortest path. To be more specific, as shown in Fig. 3, e.g., when rerouting is needed for v_5, we assume p_3 and p_c are on the first shortest path, and p_3 and p_1 are on the second shortest path. Then we have $\tau_1^l = \tau_3 + \tau_c$ and $\tau_2^l = \tau_3 + \tau_1$, where τ_n is the pheromone amount on a corresponding road link. Note that we do not directly use pheromone on all links to evaluate the whole path because it is expensive to obtain the dynamic pheromone of the whole road network, which usually involves a centralized approach.

Generally, p_c has a larger pheromone amount since congestion is predicted on that link, and according to Eq. (11), p_c has a smaller probability to be chosen. We do not enforce that the upstream vehicles should not traverse p_c because it is possible that the congestion may quickly disappear (especially considering that the traffic light control strategy in Section VI may efficiently help to alleviate the traffic congestion), and completely preventing other vehicles may cause unnecessary waste of that road link.

Algorithm 1 Pheromone-Base Vehicle Rerouting

Input : G, road network; δ, congestion threshold;
R', old routes; t, current time;
l, vehicle selection parameter;
k, number of shortest paths;
Output: Road network with new pheromone G;

```
1  Update G's roads with pheromone τ(p, t+1);
2  Find congested links p ∈ P_con by τ(p, t+1) > δ;
3  while #P_con > 0 do
4      Find road p ∈ P_con with maximum τ(p, t+1);
5      Get neighboring links P_nei connected to road p
       according to l;
6      for p' ∈ P_nei do
7          Get the vehicles Ω which need rerouting on link p'
           according to their original intentions to traverse p;
8          for υ ∈ Ω do
9              Compute k-shortest path according to the global
               distance;
10             Compute probability Pb_j^υ for each of the k
               paths according to local pheromone amount on
               the first l downstream links;
11             Randomly select one path R_j according to Pb_j^υ;
12             Set R_j as υ's new route;
13             Update pheromone τ_2(p', t+1);
14         Update pheromone τ(p', t+1);
15     Delete the checked road P_con = P_con − p;
16 Output road network with new pheromone G;
```

C. Pseudo Code

Based on the digital pheromone definition in Section. IV-A, the short-term traffic conditions can be predicted. Once a congested road link is forecasted, the roadside infrastructure will first select vehicles (i.e., locate within a range of l road links and has an original intention to traverse the congested road link) which need rerouting. Then it will search for new routes based on global distance and local dynamic pheromone for those vehicles to avoid traffic congestion. Since each vehicle randomly chooses one path out of k according to certain probabilities, this mechanism is able to avoid "road flapping" [14] where the congestion switches from one road to another when a significant number of vehicles follow the same route guidance.

The pseudo-code of the pheromone-based vehicle rerouting strategy is given in Algorithm 1. Lines 1-2 find the congested road links $p \in P_{\text{con}}$ if the pheromone of road link p is larger than the congestion threshold $\tau(p, t+1) > \delta$. In Lines 3-15, we recursively assign new routes to the concerned surrounding vehicles. In particular, Line 7 selects

the vehicles which need rerouting. Lines 9-12 combines the global distance and the local dynamic traffic pheromone to compute the new route R_j on road network G. Line 13 reports the new intention pheromone $\tau_2(p', t+1)$ to local roadside infrastructures. Line 15 updates the congested roads $p \in P_{\text{con}}$ by deleting the checked road $P_{\text{con}} = P_{\text{con}} - p$. When all the congested roads have been checked ($\#P_{\text{con}} == 0$), the algorithm outputs the road network G in Line 16.

VI. Pheromone-Based Traffic Light Control

Besides vehicle rerouting, traffic light control can also help to further alleviate traffic congestion.

A. Traffic Light Control

In a transportation system, traffic lights are signaling devices positioned at road intersections to control competing traffic flows [18]. In general, traffic light control includes two major parts: color phase and time duration. The color phase is a sequence of standard colors (i.e., red, yellow and green). The time duration describes the displaying periods of the color phases.

In the unified traffic management framework, we propose two online traffic light control strategies. Both of the two strategies automatically set color phases and calculate the time duration of these phases on competing roads according to the amount of digital pheromone. The major difference between the two strategies is whether the concerned traffic light agent considers the downstream traffic. In both strategies, we assume that each traffic light agent by default has the knowledge of its direct upstream pheromone, which can be easily obtained from corresponding roadside infrastructure agents. Traffic light agent can obtain the downstream pheromone by communicating with the neighboring traffic light agents.

B. TLC Not Considering Downstream Traffic (TLC-NCDT)

Take Fig. 4 as an example, and suppose that the pheromone information on road links p_1 and p_2 is available when computing the duration for traffic lights TL_1 and TL_2. Also assume that p_1, p_2 are one-way roads, thus the two roads have the competing relationship, where only one of the roads can be switched to green traffic lights at any time point. Based on their pheromone, for example $\tau(p_1, t+1) > \tau(p_2, t+1)$, road p_1 should be assigned the green traffic light, and road p_2 is red.

To fully utilize road capacities, we assume the time duration of the green traffic light for road p_1, denoted as $T_g(p_1)$, satisfies [41]:

$$\tau(p_1, t+1) \times \left(1 - \frac{T_g(p_1) V_f(p_1)}{L_{p_1}}\right) = \tau(p_2, t+1), \quad (12)$$

where $\frac{T_g(p_1) V_f(p_1)}{L_{p_1}}$ is the proportion of decreasing road coverage rate when cars on road p_1 travel at the free speed $V_f(p_1)$ within time duration $T_g(p_1)$. Here, the unit for T_g is second, V_f is m/s, and L_p is meter, so all units would be canceled out in $\frac{T_g(p_1) V_f(p_1)}{L_{p_1}}$. Eq. (12) indicates that the road coverage rate of road p_1 would be the same as the value of road p_2 after time duration $T_g(p_1)$, which also indicates that green light phase

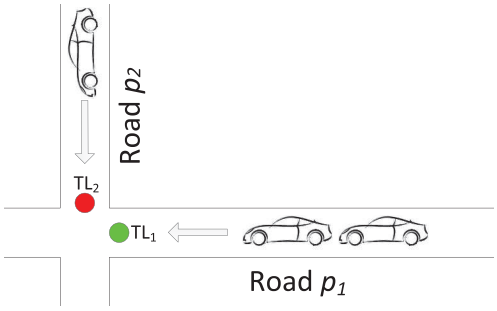

Fig. 4. Pheromone-based traffic light control not considering downstream traffic.

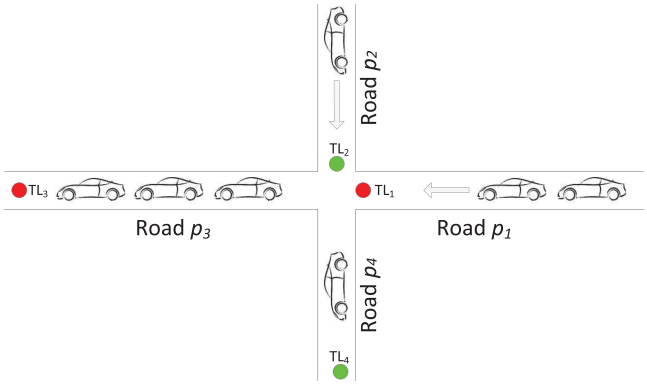

Fig. 5. Pheromone-based traffic light control considering downstream traffic.

and longer time duration should always be given to the road with larger pheromone amount. Then, based on Eq. (12), the time duration of the green traffic light on road p_1 is calculated as follows:

$$T_g(p_1) = \frac{L_{p_1} \times [\tau(p_1, t+1) - \tau(p_2, t+1)]}{V_f(p_1) \times \tau(p_1, t+1)}. \quad (13)$$

At the same time, the time duration of the red traffic light on road p_2 is set as $T_r(p_2) = T_g(p_1)$.

C. TLC Considering Downstream Traffic (TLC-CDT)

Take Fig. 5 as an example, and suppose that when regulating TL_1 and TL_2, the pheromone information on road links p_3 and p_4 can also be known through communication.

To better illustrate the idea, we assume that vehicles on p_1 and p_2 respectively go straight to the road links p_3 and p_4 (e.g., not turning right or left). Since a concerned traffic light agent always controls whether the upstream vehicles should proceed to the downstream links, it will affect the traffic on both links. Generally, distributing vehicles to downstream road links without any restriction, may deteriorate the traffic, especially if the downstream road is already congested. It is therefore desirable to also take the downstream traffic into account [42]. As shown in Fig. 5, according to the TLC-NCTD strategy in Section VI-D, TL_1 should be assigned green light with longer duration since the corresponding pheromone amount is comparatively large. However, the pheromone amount on the downstream link p_3 is also large, and longer green duration for TL_1 may make the traffic on p_3 much worse. Consequently, in this case, p_1 has a

competing relationship with p_2 as well as p_3. Similarly, p_2 has a competing relationship with p_1 as well as p_4.

Therefore, if the combination of pheromone amount on p_1 and p_4 is larger than that of p_2 and p_3, the competing relationship in TLC-CDT strategy can be formulated as:

$$[(1-\beta)\cdot\tau(p_1,t+1)+\beta\cdot\tau(p_4,t+1)] \times(1-\frac{T_g(p_1)V_f(p_1)}{L_{p_1}}) = (1-\beta)\cdot\tau(p_2,t+1) + \beta\cdot\tau(p_3,t+1). \quad (14)$$

where $\beta \in [0, 0.5]$, is the weight for downstream pheromone. Eq. (14) is similar with Eq. (12). The only difference is that there is one more weighted item on each side of the two competing components. So, we solve $T_g(p_1)$ as follows:

$$T_g(p_1) = [1-\frac{(1-\beta)\cdot\tau(p_2,t+1)+\beta\cdot\tau(p_3,t+1)}{(1-\beta)\cdot\tau(p_1,t+1)+\beta\cdot\tau(p_4,t+1)}]\times\frac{L_{p_1}}{V_f(p_1)}. \quad (15)$$

At the same time, the time duration of the red traffic light on road p_2 is set as $T_r(p_2) = T_g(p_1)$.

D. TLC Extension

In both TLC-NCDT and TLC-CDT, to avoid the situations where traffic lights change too frequently or vehicles wait too long, the time duration needs to be bounded. In our framework, if $T_g(p_1)$ is too small or too large, it is set as the default values $T_g(p_1) = 4$s or $T_g(p_1) = 120$s, respectively.

In addition, when a traffic light agent is defined to control the traffic on two-way (or multi-ways) road links, where both going straight and turning around (e.g., turning right or left) are allowed, TLC-NCDT and TLC-CDT can be easily extended to deal with this situation. We only need to dynamically recognize the upstream link and downstream link with respect to the concerned traffic light agent, and determine their competing relationships with neighbors. Then we can still employ Eq. (13) and Eq. (15) to compute the relevant green light duration.

VII. Experimentation

In this section, we compare our pheromone-based traffic management framework with existing approaches in terms of road congestion levels, travel time, air pollution and fuel consumption. We also evaluate the robustness of our framework with respect to various compliance and penetration rates.

A. Experiment Setup

The experiments are conducted on the simulation of urban mobility platform, SUMO [8]. SUMO is an open source, highly portable, microscopic and continuous traffic simulation for handling large road networks. The two testing road networks are named as Grid and Cityhall. Specifically, Grid is built by "netgenerate" tool in SUMO, which is a popular testing scenario for traffic management [7], [17], [31]. Cityhall is downloaded from OpenStreetMap,[2] which is the downtown area of Singapore. Each road in these two maps has 2 lanes. Their maps are given in Fig. 6. The road properties are summarized in Table I.

[2]http://www.openstreetmap.org with (south, west, north, east) = (1.2904, 103.8505, 1.2963, 103.8560)

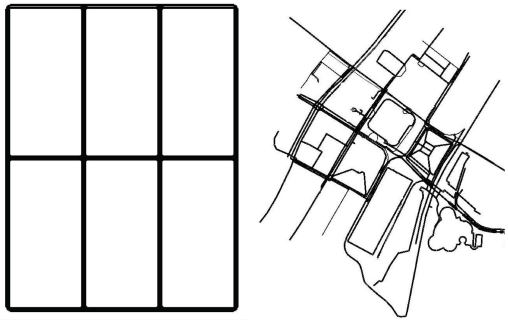

(a) (b)

Fig. 6. Two testing road networks. (a) Grid. (b) Cityhall.

TABLE I
PROPERTIES OF TESTING ROAD NETWORKS

	Grid	Cityhall
Network Area	120,000m^2	65,300m^2
Number of Roads	34	507
Length of Roads	4,701m	69,453.8m
Number of Traffic Lights	16	30

The library of TraCI [43] provides extensive commands to control the behaviors of vehicle rerouting and manage the traffic lights. In comparison to Grid, vehicle rerouting and traffic light control are more difficult in Cityhall since it involves complex roads and many traffic lights. Specifically, the configurations of vehicles for rerouting are as follows:

1) The length of vehicle is 5m, the minimal gap is 2.5m, and the vehicle following model is Krauss [8].
2) The number of vehicles are 2,000 and 800 for Grid and Cityhall, respectively.
3) The trips are randomly generated and their default routes are initialized by "duarouter" in SUMO.
4) When a vehicle arrives its destination, it will park and not occupy the road resource.
5) The congestion threshold is $\delta = 0.5$, vehicle selection parameter is $l = 3$ (explanation can be found in Section VII-B), and the number of shortest paths is $k = 5$.
6) The parameters of ϵ-SVR in LIBSVM are: $C = 10$ and RBF kernel with $\gamma = 0.3$.

In addition, the maximum simulation time is 2,000s. We run all the following experiments for 1,000 times, and record the average. In all following methods that do not dynamically change the traffic light duration, we simply apply that $T_g = T_r = 25$s for each traffic light device.

To compare different traffic management approaches, five metrics are designed as: 1) the number of congested roads, $\tau_1(p,t) > \delta$; 2) the mean and standard deviation of road coverage rate, $\tau_1(p,t)$; 3) the number of vehicles that arrived their destinations; 4) the mean travel time of the arrived vehicles; and 5) air pollution and fuel consumption. The first two metrics are introduced to assess the quality of road networks, the next two metrics are defined to evaluate diver experience, and the last one is used for testing environmental impact.

TABLE II

THE REROUTING ALGORITHM WITH DIFFERENT CONGESTION THRESHOLDS AND VEHICLE SELECTION PARAMETERS

	Grid		Cityhall	
	Rd. Cvrg. Rt	#Rerouting	Rd. Cvrg. Rt	#Rerouting
$\delta = 0.4, l = 2$	0.381±0.072	643	0.241±0.110	1916
$\delta = 0.4, l = 3$	0.365±0.069	692	0.233±0.095	1946
$\delta = 0.4, l = 4$	**0.344±0.160**	716	0.228±0.096	1973
$\delta = 0.6, l = 2$	0.407±0.075	308	0.234±0.043	1108
$\delta = 0.6, l = 3$	0.382±0.081	365	0.228±0.035	1251
$\delta = 0.6, l = 4$	0.369±0.065	422	**0.219±0.032**	1293
$\delta = 0.8, l = 2$	0.412±0.101	153	0.263±0.105	598
$\delta = 0.8, l = 3$	0.395±0.104	192	0.254±0.089	665
$\delta = 0.8, l = 4$	0.381±0.095	243	0.231±0.058	692
$\delta = 1.0, l = 2$	0.417±0.205	0	0.266±0.187	0
$\delta = 1.0, l = 3$	0.399±0.195	0	0.257±0.162	0
$\delta = 1.0, l = 4$	0.387±0.187	**0**	0.245±0.143	**0**

*Rd. Cvrg. Rt: road coverage rate

B. Vehicle Rerouting Evaluation

The pheromone-based vehicle rerouting involves several important parameters, and in this section, we investigate their influence to the performance.

1) Evaluation of Congestion Threshold and Vehicle Selection Parameter: To investigate the influence of congestion threshold δ and vehicle selection parameter l, we test the proposed rerouting strategy with $\delta \in \{0.4, 0.6, 0.8, 1.0\}$ and $l \in \{2, 3, 4\}$ on the two road networks. Road coverage rate and rerouting count (the number of rerouting occurrence) are used as the metrics. It is noted here that in this scenario, we use fixed light duration as the TLC strategy, and SVR model in Eq. (8) as the prediction model. The results are shown in Table II.

From Table II, we observe that the proposed vehicle rerouting strategy with $\delta \in \{0.4, 0.6\}$ and $l = 4$ obtains small mean traffic densities, i.e., 0.344 and 0.219 respectively for the two road networks. This is reasonable because smaller δ will incur rerouting more frequently, and all potential congestion is likely to be prevented early. At the same time, larger l usually involves more vehicles to alleviate the congestion, therefore the mean road coverage rate is expected to be further reduced. However, smaller δ and larger l always result in large rerouting count, which is respectively 716 and 1,973 for $\delta = 0.4$ and $l = 4$ in Table II. When δ is large, the rerouting count usually becomes small, and the extreme case of $\delta = 1.0$ means that all vehicles adopt their initial routes (i.e., #Rerouting = 0). Since too many times of rerouting will disturb the driving behaviors, and to balance the road coverage rate and rerouting count, the congestion threshold is set as $\delta = 0.5$ and $l = 3$ in the following experimental studies.

2) Evaluation of Weights and Prediction Steps: Besides congestion threshold and vehicle selection parameter, in vehicle rerouting strategy, we test the weight of pheromone against two other weights, which are length of road, and mean travel time respectively. Our pheromone-based models, which use Eq. (5) and Eq. (8) to predict the traffic condition, are respectively indicated as "Pheromone τ-Fusion" and "Pheromone τ-SVR."

TABLE III

VEHICLE REROUTING RESULTS WITH VARIOUS WEIGHTS AND PREDICTION STEPS

	#Con. Roads	Rd. Cvrg. Rt	#Arr. Vehs	Travel Time
Grid Network				
Length	20.6	0.670±0.197	531	310.3
Mean Travel Time	11.9	0.501±0.257	1309	253.1
Pheromone τ-Fusion	8.7	0.372±0.212	1616	209.9
Pheromone τ-SVR	8.8	0.374±0.226	1620	208.7
Pheromone τ-Fusion-1	7.3	0.325±0.219	1675	199.3
Pheromone τ-SVR-1	6.7	0.313±0.251	1680	190.7
Pheromone τ-Fusion-2	5.8	0.309±0.231	1687	187.9
Pheromone τ-SVR-2	**5.4**	**0.293±0.219**	**1705**	**181.2**
Pheromone τ-Fusion-3	6.5	0.306±0.241	1685	189.4
Pheromone τ-SVR-3	6.1	0.301±0.218	1697	186.6
Pheromone τ-Fusion-4	8.4	0.321±0.262	1661	208.1
Pheromone τ-SVR-4	7.6	0.312±0.234	1673	203.7
Cityhall Network				
Length	19.2	0.293±0.261	421	577.9
Mean Travel Time	14.6	0.268±0.225	486	471.6
Pheromone τ-Fusion	11.9	0.232±0.126	569	455.7
Pheromone τ-SVR	11.9	0.230±0.181	564	453.4
Pheromone τ-Fusion-1	10.6	0.220±0.101	582	450.3
Pheromone τ-SVR-1	10.1	0.214±0.132	597	448.1
Pheromone τ-Fusion-2	9.9	0.206±0.112	606	437.5
Pheromone τ-SVR-2	**9.4**	**0.195±0.130**	**631**	**435.2**
Pheromone τ-Fusion-3	10.8	0.215±0.106	598	444.4
Pheromone τ-SVR-3	10.1	0.209±0.108	603	439.2
Pheromone τ-Fusion-4	12.8	0.231±0.120	573	451.7
Pheromone τ-SVR-4	11.7	0.224±0.149	582	447.2

*Con. Roads: congested roads, Arr. Vehs: arrived vehicles
Rd. Cvrg. Rt: road coverage rate

To further evaluate the influence of prediction steps in the two pheromone-based models, we also try different m in Eq. (9) and Eq. (10), which are respectively indicated as "Pheromone τ-Fusion-m" and "Pheromone τ-SVR-m" ("Pheromone τ-Fusion-m" is equal to "Pheromone τ-Fusion" if $k = 0$, and the same holds for "Pheromone τ-SVR-m"). We note that, in this scenario, we again employ fixed light duration as the TLC strategy. In addition, we use congested road count, mean road coverage rate, arrived vehicles and mean travel time as four metrics, and all the results are recorded in Table III.

From Table III, we observe that the two pheromone-based rerouting algorithms report superior results to the other two with different weights. In particular, the first weight only utilizes the length of road p (i.e., L_p) while ignoring dynamic traffic conditions. The mean travel time is designed as $\frac{L_p}{\bar{V}(p,t)}$, which adopts the mean speed $\bar{V}(p,t)$. In comparison with them, the pheromone $\tau(p, t+1)$ is able to forecast traffic densities by involving drivers' route intentions $\tau_2(p, t+1)$. In addition, among all the pheromone-based rerouting algorithms, the performance becomes better as prediction step m increases up to 2, and deteriorates afterwards. This is because, if the prediction interval is comparatively longer, the framework has sufficient time to prevent the traffic congestion from happening. However, if the prediction period is too long, the prediction accuracy may decrease, which will result in undesirable performance for rerouting. On the other hand, comparing the two pheromone-based rerouting algorithms, we notice that "Pheromone τ-Fusion-m" is only competitive to "Pheromone τ-SVR-m" for $m = 0$, and "Pheromone τ-SVR-m" is always better than "Pheromone τ-Fusion-m" for all other cases (i.e., $m = 1, 2, 3,$ and 4). This is rational

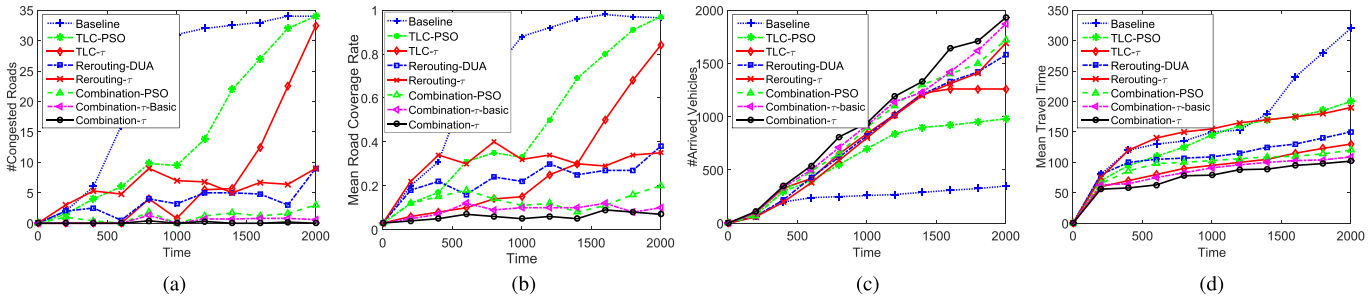

Fig. 7. Results on the *Grid* network by vehicle rerouting and traffic light control (TLC). (a) Congested roads. (b) Mean road coverage rate. (c) Arrived vehicles. (d) Mean travel time.

TABLE IV
RESULTS BY VARIOUS TRAFFIC LIGHT CONTROL STRATEGIES

	#Con. Roads	Rd. Cvrg. Rt	#Arr. Vehs	Travel Time
Grid Network				
TLC-Fixed	23.5	0.708±0.265	341	328.3
TLC-NCDT	8.6	0.296±0.243	1190	138.9
TLC-CDT	**7.5**	**0.278±0.191**	**1269**	**124.6**
Cityhall Network				
TLC-Fixed	21.9	0.324±0.377	451	452.4
TLC-NCDT	10.8	0.249±0.214	510	382.2
TLC-CDT	**9.3**	**0.228±0.193**	**539**	**373.0**

*Con. Roads: congested roads, Arr. Vehs: arrived vehicles
Rd. Cvrg. Rt: road coverage rate

because if $m = 0$, only extremely short-term prediction is required, and both models can provide satisfactory results. As m increases, SVR can achieve more accurate results with respect to comparatively long term prediction, because some delicate learning algorithms are used in SVR.

C. Traffic Light Control Evaluation

Two different dynamic strategies are proposed for TLC in Section VI: the first one is TLC not considering downstream traffic (TLC-NCDT), and the second one is TLC considering the downstream traffic (TLC-CDT). In this section, we test the two dynamic strategies against the one with fixed light duration (TLC-Fixed). To better evaluate the effect of these two strategies, we do not employ any rerouting algorithm, and we also keep the prediction step $m = 0$. In addition, we use the same four metrics in Table III, and all the results are recorded in Table IV.

From Table IV, we observe that the two dynamic TLC strategies are always better than the fixed light duration strategy on both road networks. This is reasonable because TLC-NCDT and TLC-CDT always dynamically regulate the light period according to the traffic situation, which can meet the actual traffic demand better. Comparing the two dynamic strategies, TLC-CDT is always superior to TLC-NCDT. This difference comes from the fact that TLC-NCDT does not consider the downstream traffic, and more often than not, distributing vehicles to downstream road without any restriction, may deteriorate the traffic, especially if the downstream road is already congested. Therefore, considering the traffic both on upstream and downstream roads for the traffic light agents will help to improve the traffic.

Among all rerouting algorithms in Table III and all TLC strategies in Table IV, "Pheromone τ-SVR-2" and TLC-CDT respectively achieve the best performance, hence it is desirable to combine them as the framework of traffic management.

D. Overall Performance of the Proposed Framework

In the last two subsections, we have evaluated the vehicle rerouting strategy and the traffic light control policy respectively. In this section, we combine the vehicle rerouting algorithm "Pheromone τ-SVR-2" and the traffic light control strategy TLC-CDT as our framework of traffic management, which is denoted as Combination-τ.

Then we compare the performance of the proposed framework with seven other traffic management approaches:

1) Baseline, without controlling routes or traffic signals (i.e., fixed color phases and time durations);
2) TLC-PSO, traffic light control by particle swarm optimization [18];
3) TLC-τ, pheromone-based traffic light control strategy, which is equal to TLC-CDT in Section VII-C;
4) Rerouting-DUA (dynamic user assignment),[3] by far the best rerouting algorithm to obtain stochastic user-equilibrium traffic states [14];
5) Rerouting-τ, pheromone-based rerouting approach, which is equal to "Pheromone τ-SVR-2" in Section VII-B;
6) Combination-PSO, the combination of vehicle rerouting and traffic light control by PSO [1];
7) Combination-τ-basic, combination of vehicle rerouting algorithm "Pheromone τ-SVR" in Section VII-B and the traffic light control strategy TLC-NCDT in Section VII-C.

We use the same four metrics as shown in Table III, and all results for the two road networks are shown in Fig. 7 and Fig. 8 respectively. Additionally, the corresponding overall mean value is also recorded in Table V.

Figs. 7-8 show the results of all traffic management approaches on Grid and Cityhall, respectively, which plot the average over 1,000 times, with an interval of 200 seconds. The two traffic light control methods (i.e., TLC-τ and TLC-PSO) give better results than Baseline in terms of the four metrics. In addition, pheromone-based traffic light control (TLC-τ) is superior to TLC-PSO. For instance, in Table V, the average numbers of congested roads by TLC-PSO and TLC-τ are 14.5 and 7.6 on Grid, respectively. For Cityhall, these values by TLC-PSO and TLC-τ are 15.6 and 9.7, respectively.

[3]http://sumo-sim.org/userdoc/Tools/Assign.html

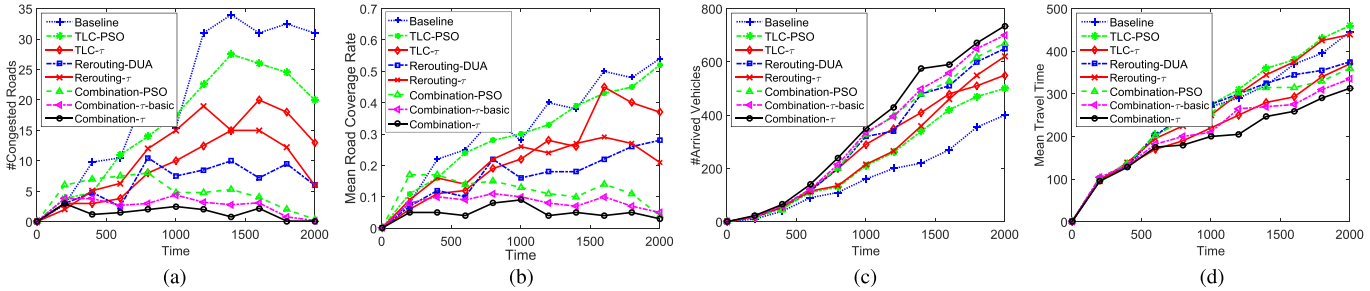

Fig. 8. Results on the *Cityhall* network by vehicle rerouting and traffic light control (TLC). (a) Congested roads. (b) Mean road coverage rate. (c) Arrived vehicles. (d) Mean travel time.

In particular, TLC-PSO only aims to optimize the time duration for the fixed color phases. On the contrary, TLC-τ dynamically sets color phases and time duration to roads according to the predicted traffic densities. In comparison to Baseline, the number of arrived vehicles by TLC-τ increases from 353 to 1260 on Grid network, and improves from 402 to 551 on Cityhall network. Due to the better traffic conditions, the mean road coverage rate and the mean travel time by TLC-τ decrease significantly than those of Baseline.

The two vehicle rerouting algorithms obtain better results than the Baseline, TLC-PSO and TLC-τ, with respect to most of the performance metrics. For instance, in Fig. 7(a), TLC-τ arrives at the similar number of congested roads with Rerouting-DUA and Rerouting-τ before 1,400s, whereas reports poor results after 1,400s when the traffic volume increases. To explain, the vehicles are randomly scattered at the beginning, and they are likely to form traffic flows as time passes, which will compete for the green light duration with each other. TLC-τ assigns the default time of green traffic lights (i.e., $T_g = 4$s) to two competing roads with similar traffic densities. Thus, TLC-τ is more suitable to the unbalance traffic scenarios. On the other hand, Rerouting-DUA is slightly better than Rerouting-τ in terms of the four metrics. For instance, in Table V, the mean traffic densities by Rerouting-DUA and Rerouting-τ are 0.268 and 0.294 on Grid, respectively. In essential, Rerouting-DUA is an offline algorithm, which evaluates the traffic condition after vehicles have traveled through all candidate routes. Thus, it is only designed for simulation because vehicles' movement in realistic transportation systems is irrevocable. Although our Rerouting-τ is designed as an online algorithm, it achieves the competitive results compared to Rerouting-DUA.

Furthermore, the three approaches (i.e., Combination-PSO, Combination-τ-basic, and Combination-τ) combining vehicle rerouting and traffic light control yield better results on average than other five algorithms, in terms of the four metrics. In addition, the Combination-τ-basic is superior to Combination-PSO, because Combination-PSO does not design its two components under a unified framework to optimize them in a simultaneous manner. In Table V, road conditions become better when using Combination-τ-basic. The average numbers of congested roads on Grid and Cityhall are 0.5 and 2.6, respectively. However, by improving each component in Combination-τ-basic, our Combination-τ achieves much better result than all other approaches, e.g.,

TABLE V

RESULTS ON TWO ROAD NETWORKS BY VEHICLE REROUTING AND TRAFFIC LIGHT CONTROL (TLC)

	#Con. Roads	Rd. Cvrg. Rt	#Arr. Vehs	Travel Time
Grid Network				
Baseline	22.2	0.690±0.173	353	319.5
TLC–PSO	14.5	0.471±0.246	981	201.2
TLC–τ	7.6	0.285±0.217	1260	130.6
Rerouting–DUA	3.5	0.268±0.198	1583	149.8
Rerouting–τ	5.7	0.294±0.232	1690	188.9
Combination–PSO	1.1	0.127±0.146	1725	119.5
Combination–τ–Basic	0.5	0.087±0.027	1871	108.9
Combination–τ	**0.1**	**0.059±0.029**	**1930**	**103.6**
Cityhall Network				
Baseline	20.0	0.316±0.158	402	445.3
TLC–PSO	15.6	0.292±0.153	506	461.2
TLC–τ	9.7	0.224±0.110	551	371.1
Rerouting–DUA	6.3	0.163±0.096	654	375.2
Rerouting-τ	9.8	0.196±0.120	621	439.6
Combination–PSO	4.5	0.115±0.091	679	360.2
Combination–τ–basic	2.6	0.078±0.038	708	325.9
Combination–τ	**1.4**	**0.047±0.021**	**736**	**313.4**

*Con. Roads: congested roads, Arr. Vehs: arrived vehicles
Rd. Cvrg. Rt: road coverage rate

the mean traffic densities on two road networks reduce to 0.1 and 1.4, respectively. Moreover, driver experience is also increased through our framework. the numbers of arrived vehicles on Grid and Cityhall are 1,930 and 736, respectively. The mean travel time on two road networks decreases to 101.6s and 313.4s, respectively. These results indicate that our traffic management framework is effective for improving the quality of road networks, and efficient in saving travel time. On the other hand, the results of Combination-τ is dominantly better than that of Rerouting-τ and TLC-τ, which further justifies the combination of pheromone-based vehicle rerouting and traffic light control.

We also investigate the average duration, maximum duration and minimum duration of green color for each traffic light in our Combination-τ approach. The results on two test networks are shown in Fig. 9(a) and (b) respectively. We observe that, on both networks, our TLC-CDT strategy is able to dynamically change the duration of green color according to pheromone amount, since the average green duration varies with different traffic lights, which also justifies that pheromone is able to represent the dynamic traffic load well. From maximum duration and minimum duration, we notice that, some of the traffic lights reach the upper bound (120s) or lower bound (4s), which justifies the feasibility of the two bounds.

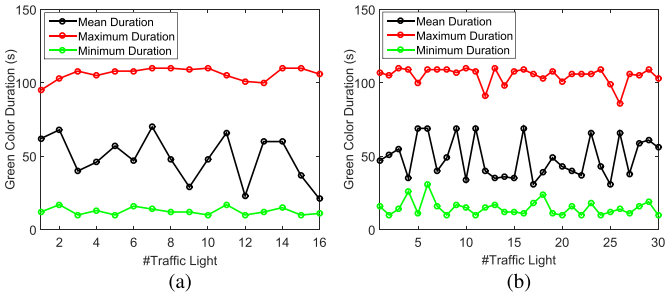

Fig. 9. Green color duration by TLC-CDT

TABLE VI
RESULTS OF AIR POLLUTION AND FUEL CONSUMPTION

	Grid		Cityhall	
	CO_2 (mg)	Fuel (ml)	CO_2 (mg)	Fuel (ml)
Baseline	5.521e+008	2.214e+005	5.512e+008	2.113e+005
TLC–PSO	4.089e+008	1.685e+005	5.239e+008	2.094e+005
TLC–τ	4.025e+008	1.591e+005	5.201e+008	2.011e+005
Rerouting–DUA	3.268e+008	1.323e+005	4.588e+008	1.887e+005
Rerouting–τ	3.824e+008	1.502e+005	5.009e+008	2.038e+005
Combination–PSO	2.897e+008	1.157e+005	4.398e+008	1.749e+005
Combination–τ–basic	2.739e+008	1.116e+005	4.327e+008	1.727e+005
Combination–τ	**2.675e+008**	**1.086e+005**	**4.309e+008**	**1.710e+005**

E. Auxiliary Performance Evaluation

Although the proposed framework targets at reducing road network's overall congestion levels, we can also expect that the framework can reduce the overall air pollution levels and fuel consumption as well. The apparent reason is that reducing road congestion can naturally decrease CO_2 emissions and reduce fuel consumption.

In this section, we compare the air pollution (i.e., CO_2) and fuel consumption of the traffic management framework against other approaches,[4] the result of which are reported in Table VI.

From Table VI, we can see that the three combination approaches (i.e., Combination-PSO, Combination-τ-basic and Combination-τ) are superior to the other five approaches, and our traffic management framework (i.e., Combination-τ) achieves the best results. In particular, the CO_2 emission and fuel consumption by our framework on Grid are 2.675e+8mg and 1.086e+5ml, respectively. These values are 4.309e+8mg and 1.710e+5ml on Cityhall, respectively. These results demonstrate that our traffic management framework is beneficial for reducing air pollution and saving energy consumption.

F. Robustness Evaluation

The performance of any proposed approach/framework should be gauged by not only the targeted performance metrics (e.g., number of congested links and air pollution level in our case), but also the robustness under various uncertainties, i.e., robustness against inherent parameter variations. Therefore, in the next two subsections, we will evaluate the robustness performance of our framework against two key parameters, i.e., compliance rate and penetration rate.

[4]We note here that these two metrics can be directly acquired from the built-in functions of SUMO.

TABLE VII
RESULTS BY PHEROMONE-BASED VEHICLE REROUTING WITH DIFFERENT COMPLIANCE RATES ($R_c \in [0, 1]$)

	#Con. Roads	Rd. Cvrg. Rt	#Arr. Vehs	Travel Time
Grid Network				
$R_c = 0.0$	22.2	0.690±0.173	353	319.5
$R_c = 0.2$	21.3	0.651±0.167	483	287.0
$R_c = 0.4$	16.9	0.559±0.179	739	248.5
$R_c = 0.6$	10.9	0.418±0.205	1173	228.5
$R_c = 0.8$	6.4	0.242±0.194	1629	195.1
$R_c = 1.0$	**5.7**	**0.294±0.232**	**1690**	**188.9**
Cityhall Network				
$R_c = 0.0$	20.0	0.316±0.151	402	445.3
$R_c = 0.2$	19.3	0.292±0.186	463	440.6
$R_c = 0.4$	16.7	0.275±0.177	482	439.9
$R_c = 0.6$	14.2	0.239±0.168	532	**429.7**
$R_c = 0.8$	11.8	0.214±0.136	589	437.5
$R_c = 1.0$	**9.8**	**0.196±0.120**	**621**	439.6

*Con. Roads: congested roads, Arr. Vehs: arrived vehicles, Rd. Cvrg. Rt: road coverage rate

TABLE VIII
RESULTS BY PHEROMONE-BASED VEHICLE REROUTING WITH DIFFERENT PENETRATION RATES ($R_p \in [0, 1]$)

	#Con. Roads	Rd. Cvrg. Rt	#Arr. Vehs	Travel Time
Grid Network				
$R_p = 0.0$	9.0	0.341±0.159	1672	216.0
$R_p = 0.2$	8.3	0.333±0.142	1684	209.5
$R_p = 0.4$	7.7	0.322±0.149	1687	202.3
$R_p = 0.6$	6.9	0.314±0.162	**1699**	195.1
$R_p = 0.8$	6.4	0.307±0.155	1688	199.3
$R_p = 1.0$	**5.7**	**0.294±0.232**	1690	**188.9**
Cityhall Network				
$R_p = 0.0$	12.4	0.224±0.135	581	468.6
$R_p = 0.2$	11.6	0.213±0.114	588	459.8
$R_p = 0.4$	10.5	**0.194±0.119**	609	457.2
$R_p = 0.6$	11.3	0.210±0.142	605	453.3
$R_p = 0.8$	10.8	0.208±0.132	614	447.1
$R_p = 1.0$	**9.8**	0.196±0.120	**621**	**439.6**

*Con. Roads: congested roads, Arr. Vehs: arrived vehicles Rd. Cvrg. Rt: road coverage rate

1) Robustness Against Different Compliance Rates: In this section, we test our pheromone-based vehicle rerouting algorithm with different compliance rates ($R_c \in [0, 1]$). The compliance rate means the percentage of drivers who will follow navigation guidance provided by Rerouting-τ.

In Table VII, our Rerouting-τ with $R_c \in [0.8, 1.0]$ only brings 6.4/34 = 18.8% and 11.8/507 = 2.3% congested roads on Grid and Cityhall, respectively. In addition, our rerouting algorithm with $R_c \in [0.8, 1.0]$ reports competitive results in terms of the other three metrics. These results indicate that our pheromone-based vehicle rerouting algorithm is robust to the compliance rates of $[0.8, 1.0]$.

2) Robustness Against Different Penetration Rates: In this section, we test our pheromone-based vehicle rerouting algorithm with various penetration rates ($R_p \in [0, 1]$). The penetration rate defines the percentage of drivers who will share their route information (intention pheromone τ_2 in Eq. (2)) to the local roadside infrastructures.

In Table VIII, our Rerouting-τ with $R_p \in [0.6, 1.0]$ only causes 6.9/34 = 20.3% and 11.3/507 = 2.2% congested roads on Grid and Cityhall, respectively. When $R_p \in [0.6, 1.0]$, our rerouting algorithm obtains competitive results in terms of other three metrics. This demonstrates that our pheromone-based vehicle rerouting algorithm is robust to the penetration rates of $[0.6, 1.0]$.

TABLE IX
MEAN TRAVEL TIME (S) WITH MULTIPLE ITERATIONS

Q	1	**2**	3	4	5	6	7
Grid	102.3	97.6	96.4	94.5	104.2	95.8	102.9
Cityhall	313.4	306.7	309.5	315.2	316.8	304.8	314.8

VIII. FURTHER IMPROVEMENTS

In this section, we propose two improvements regarding our pheromone based framework. First, we consider multiple interactions between vehicle rerouting and traffic light control to achieve better system performance. Second, we increase the lower bound of green light duration and allow for yellow lights and all-red lights, to make our framework more realistic.

A. Iterative Interaction Between Vehicle Rerouting and Traffic Light Control

In the proposed framework (see Fig 1), traffic light timing is always dynamically regulated according to the latest pheromone (i.e., traffic pheromone and intention pheromone) on corresponding road links, and the vehicle rerouting strategy is activated only when potential congestion is detected. Once their new routes are determined by the rerouting strategy, the intention pheromone on relevant road links will be updated timely, and traffic light timing will be calculated based on the latest pheromone. However, it is more attractive to investigate the interactions between vehicle rerouting and traffic light control for multiple iterations. To achieve this, we first perform the vehicle rerouting strategy based on Eq. (11) to update routes for selected vehicles, then traffic light timing will be computed. Since some vehicles change their routes, the pheromone in Eq. (11) will also be updated. Therefore, it is reasonable to perform vehicle rerouting again and calculate new traffic light timing. We repeat the iterations for Q times to investigate relevant performance. Moreover, we only take the final mean travel time on both networks as measurement, and Q is from 1 to 7, the results of which are recorded in Table IX.

We would like to point out that, when $Q = 1$, the method is exactly our Combination-τ approach. From Table IX we see that, the mean travel time varies with Q on both networks. Pertaining to all selected Q values, the minimal mean travel time is 94.5s on Grid network as $Q = 4$, and 304.8s on Cityhall network as $Q = 6$ respectively, both of which are lower than that of the original Combination-τ approach. It is worth noting that we cannot guarantee a consistent total travel time decrease as the number of iteration increases in this special case. In practice, we can iterate the interaction process for several times, and select the policy with the best overall performance, i.e., total travel time, as the output.

B. Regulating Lower Bound of Green Light Duration and Allowing for Yellow Lights and All-Red Lights

In our pheromone based framework, the traffic light duration dynamically changes with the amount of pheromone on relevant road links. We set the lower bound of green light duration to be 4 seconds (see Section VI-D) purely from the computational perspective. However, from practical perspective, it would be more realistic to increase this lower bound. Thus, we investigate the system metrics against this lower bound, i.e., from 4 seconds to 14 seconds with an interval of 2 seconds, on the two road networks. For simplification, we only choose the metrics of arrived vehicles and mean travel time at the last simulation step. Accordingly, we plot the results in Fig. 10.

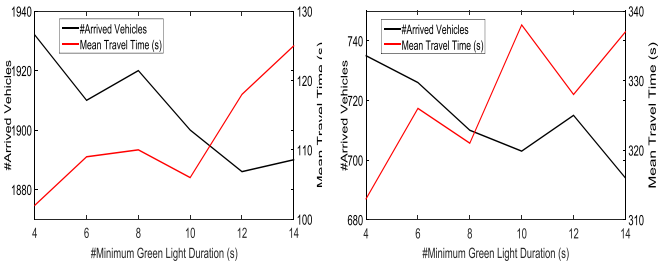

Fig. 10. Regulating the lower bound of green light duration. (a) Grid network. (b) Cityhall network.

TABLE X
RESULTS FOR YELLOW LIGHTS AND ALL-RED LIGHTS

	# Arrived Vehicles		Mean Travel Time (s)	
	Yellow(0s), All-red (0s)	Yellow(3s), All-red (2s)	Yellow(0s), All-red (0s)	Yellow(3s), All-red (2s)
Grid	1904	1893	106.3	109.5
Cityhall	711	703	322.8	328.5

From Fig. 10 we see that generally, the amount of arrived vehicles will decrease and the mean travel time will increase as the minimum green duration becomes longer on the two road networks. This happens because in our approach, to balance the traffic on competing road links, the calculated green light duration is theoretically possible, although rarely, to reach below 4 seconds, which can also be observed from Fig. 9. In that case, if we increase this lower bound, a waste of green duration might happen, and an adverse increase of red light duration on corresponding competing road links would probably arise. However, to make the green light duration realistic and maintain favorable system metrics, we may choose 10 seconds on Grid network (see Fig. 10(a)) and 8 seconds on Cityhall network (see Fig. 10(b)) as the lower bounds of green duration respectively, which are still superior to other methods as shown in Fig. 7 and Fig. 8.

In addition, we also study the cases of yellow lights and all-red lights in our pheromone based framework. Particularly, we enforce the last 3 seconds of the calculated green duration to be yellow duration, and the first 2 seconds of the calculated green duration to be red duration (thus all-red would happen). During the yellow light, the vehicles are allowed to pass through the intersection if they are within triple vehicle lengths before the stopping line. Moreover, we adopt 10 seconds on Grid network and 8 seconds on Cityhall network as the lower bounds of green duration respectively. Again, we focus on the metrics of arrived vehicles and mean travel time at the last simulation step, which are recorded in Table X. We would like to note that "Yellow (0s), All-red (0s)" on the two road networks correspond to our original approach which did not consider the cases of yellow lights and all-red lights.

From Table X we observe that the two system metrics deteriorate if we consider the cases of yellow lights and all-red lights. This happened because there would be more vehicles passing through the intersections if the lights are green during the two cases. However, this deterioration is considerably slight, e.g., the mean travel time only increases about 3 seconds for the Grid network. It is rationale since generally the yellow duration and all-red duration only occupy a small portion of the calculated green duration. Moreover, vehicles may still be able to pass through the intersections even in yellow light duration. Thus, the results in Table X justify that our approach is suitable for realistic situation.

IX. Discussion

It is worth noting that the modern data collection technologies make it feasible to instantiate our digital pheromone into a realistic intelligent transportation system (ITS). For instance, the basic information, such as length of vehicle L_{veh}, length of road L_p, lanes of road lanes(p), the free speed $V_f(p)$, can be obtained by vehicle manufacturers and urban planning administration. Vehicles can use the speed pulse to record their speed. Roadside infrastructures can utilize digital cameras (i.e., with computer vision techniques) to count the numbers of moving vehicles $N(p,t)$ and the halting vehicles $|\text{Halts}(p,t)|$. The intentions about which road links to enter next for vehicles can be obtained if they communicate with the local roadside infrastructure. Thus, our digital pheromone can be easily applied into ITSs. In case we cannot get the speed of each vehicle, we could adopt some machine learning techniques to learn the average speed of relevant road links by relying on sparse traffic data [44]–[46]. Regarding the vehicle counts, they might be estimated based on historical traffic data if digital camera cannot count them correctly. Further, in absence of complete vehicle intentions, we may use probabilistic inference to estimate them, or employ machine learning techniques to predict them.

Our rerouting strategy in this paper relies on the k shortest path algorithm. In some cases, two consecutive shortest paths might be very different even though the difference of travel cost is small, and the recommended path may not be accepted by user if he is not familiar with that path. However, our rerouting algorithm in this paper focuses on reducing traffic congestion so as to improve the overall traffic performance. Thus the degree of difference from original path, i.e., user preference is not our major concern in this work. We wish to note that the graphs of two testing road networks (Grid and Cityhall) in this paper are highly connected, and thus two consecutive shortest paths should always share most of the road links. Nevertheless, it is definitely worth considering the difference of consecutive shortest paths and user preference in rerouting strategy in our future work.

To better fuse the traffic pheromone and intention pheromone, we adapt SVR regression model in Section IV-B. Normally, SVR regression model is not suitable for large online system due to its computation efficiency. However, our approach is decentralized, and we use SVR to compute a regression model respectively for each involved road link, rather than for all road links together. In this case, regression model of each road link can be efficiently computed since there are only two variables (i.e., Eq. (6)). And the average computation time of each regression model on the two road networks is 0.085s and 0.098s respectively, which justifies its computation efficiency in our online system.

To better fuse the traffic pheromone and intention pheromone, we adapt the SVR model in Section IV-B. Normally, SVR is not very suitable for large online systems. However, our approach is decentralized, and we use SVR to compute a regression model for each involved road link, instead of all road links together. In this case, the regression model of each road link can be quickly computed since there are only two variables in Eq. (6). In our simulation, the average computation time of each regression model on the two road networks is 0.085s and 0.098s respectively, which is obviously suitable for online applications.

Two types of user equilibrium would be potentially involved in this paper: (1) Drivers will dynamically choose the paths which they consider as optimal especially when confronted with crowded or congested roads, where an equilibrium will be achieved if we do not impose any external strategies [47]. (2) When we implement our approach with multiple shots of vehicle rerouting and traffic light control, an equilibrium between vehicle rerouting and traffic light control can also be achieved. The first type of user equilibrium usually takes comparatively long time to form, because drivers always reactively switch to the optimal path according to their own observations, especially when congestion has already happened. On the contrary, the traffic condition could be predicted in our approach, and we can reroute relevant vehicles or regulate duration of relevant traffic lights in advance, to guarantee fluent traffic flow, which can be justified by the results in Section VII. Regarding the second type of user equilibrium, we preliminarily investigate it in an iterative manner to decide a satisfactory number of shots (see Section VIII-A). However, we are aware of that this type of equilibrium can be formulated and solved as an optimization problem using the knowledge of game theory [48], which would be further addressed as our future work. At the same time, it is also definitely worth investigating the trade-off between system performance and equity of individual drivers [49], since we may violate the routing intentions of some drives to achieve a better system performance.

In addition, spillbacks is a common phenomenon in traffic [26], [27]. We did not explicitly discuss it in our framework because we adopt the unified pheromone to describe the traffic conditions on each road link. We are actually alleviating the spillbacks when we consider the pheromone amount on the downstream road link with respect to the traffic light control (i.e., TLC-CDT). The experimental results showed that our approach can improve the quality of traffic, which also implies that it is able to address the issue of spillbacks. However, it is definitely worth to explicitly consider the spillbacks in our approach and compare it with other spillbacks-oriented methods in future, such as [26] and [27].

X. Conclusion and Future Work

In this paper, a novel multiagent pheromone-based traffic management framework is proposed for reducing traffic congestion, where we unify the vehicle rerouting and traffic light control for traffic congestion alleviation. In this framework, two different pheromones, i.e., traffic pheromone and intention pheromone are combined to model and predict the traffic condition. Once congestion is predicted, we first select vehicles according to the distance to the concerned road and their driving intentions, then we use one probabilistic strategy based on global distance and local pheromone to reroute those vehicles. At the same time, depending on whether or not they consider the downstream traffic condition, we develop two pheromone-based strategies to dynamically control traffic lights to further alleviate the traffic congestion. Experimental results on two road networks show the superior performance in terms of congested road units, road coverage rate, arrived vehicles, travel time, air pollution and fuel consumption. In addition, our traffic management framework is robust to various compliance and penetration rates.

In the future, we will:

- examine the performance of our framework on other complex road networks with various numbers of vehicles;
- take into account the difference of consecutive shortest paths and user preferences in vehicle rerouting strategy;
- investigate the balance between system performance and equity of individual drivers [49];
- investigate machine learning techniques to predict the incoming and outgoing vehicle information when the full information is unavailable;
- consider the more realistic use case, in which only a sparse number of road links can collect, compute, predict and report traffic pheromone information.

References

[1] A. L. C. Bazzan, D. de Oliveira, F. Klügl, and K. Nagel, "To adapt or not to adapt—Consequences of adapting driver and traffic light agents," in *Adaptive Agents and Multi-Agent Systems III. Adaptation and Multi-Agent Learning*. New York, NY, USA: Springer, 2008, pp. 1–14.

[2] USA TODAY. *The Effects of Traffic Congestion*, accessed Oct. 2014. [Online]. Available: http://traveltips.usatoday.com/effects-traffic-congestion-61043.html

[3] *TTI's 2012 Urban Mobility Report*, Texas A&M Transp. Inst., College Station, TX, USA, 2012.

[4] Z. Cao, H. Guo, J. Zhang, D. Niyato, and U. Fastenrath, "Finding the shortest path in stochastic vehicle routing: A cardinality minimization approach," *IEEE Trans. Intell. Transp. Syst.*, vol. 17, no. 6, pp. 1688–1702, Jun. 2016.

[5] D. J. Wilkie, J. P. van den Berg, M. C. Lin, and D. Manocha, "Self-aware traffic route planning," in *Proc. 25th Conf. Artif. Intell. (AAAI)*, 2011, pp. 1521–1527.

[6] Z. Cao, H. Guo, J. Zhang, D. Niyato, and U. Fastenrath, "Improving the efficiency of stochastic vehicle routing: A partial Lagrange multiplier method," *IEEE Trans. Veh. Technol.*, vol. 65, no. 6, pp. 3993–4005, Jun. 2016.

[7] J. France and A. A. Ghorbani, "A multiagent system for optimizing urban traffic," in *Proc. IEEE/WIC Int. Conf. Intell. Agent Technol. (IAT)*, Oct. 2003, pp. 411–414.

[8] M. Behrisch, L. Bieker, J. Erdmann, and D. Krajzewicz, "SUMO—Simulation of urban mobility: An overview," in *Proc. 3rd Int. Conf. Adv. Syst. Simulation (SIMUL)*, 2011, pp. 55–60.

[9] B. Chen and H. H. Cheng, "A review of the applications of agent technology in traffic and transportation systems," *IEEE Trans. Intell. Transp. Syst.*, vol. 11, no. 2, pp. 485–497, Jun. 2010.

[10] Y. Ando, Y. Fukazawa, O. Masutani, H. Iwasaki, and S. Honiden, "Performance of pheromone model for predicting traffic congestion," in *Proc. 5th Int. Joint Conf. Auto. Agents Multiagent Syst. (AAMAS)*, 2006, pp. 73–80.

[11] S. Kurihara, H. Tamaki, M. Numao, J. Yano, K. Kagawa, and T. Morita, "Traffic congestion forecasting based on pheromone communication model for intelligent transport systems," in *Proc. 11th Conf. Congr. Evol. Comput.*, 2009, pp. 2879–2884.

[12] O. Masutani, H. Sasaki, H. Iwasaki, Y. Ando, Y. Fukazawa, and S. Honiden, "Pheromone model: Application to traffic congestion prediction," in *Proc. 4th Int. Joint Conf. Auto. Agents Multiagent Syst. (AAMAS)*, 2005, pp. 1171–1172.

[13] Z. Cao, H. Guo, J. Zhang, and U. Fastenrath, "Multiagent-based route guidance for increasing the chance of arrival on time," in *Proc. 14th AAAI Conf. Artif. Intell. (AAAI)*, 2016, pp. 3814–3820.

[14] J. Pan, I. S. Popa, K. Zeitouni, and C. Borcea, "Proactive vehicular traffic rerouting for lower travel time," *IEEE Trans. Veh. Technol.*, vol. 62, no. 8, pp. 3551–3568, Oct. 2013.

[15] K. Dresner and P. Stone, "Multiagent traffic management: A reservation-based intersection control mechanism," in *Proc. 3rd Int. Joint Conf. Auto. Agents Multiagent Syst. (AAMAS)*, 2004, pp. 530–537.

[16] M. Vasirani and S. Ossowski, "A market-inspired approach to reservation-based urban road traffic management," in *Proc. 8th Int. Joint Conf. Auto. Agents Multiagent Syst. (AAMAS)*, 2009, pp. 617–624.

[17] T. Yamashita, K. Izumi, K. Kurumatani, and H. Nakashima, "Smooth traffic flow with a cooperative car navigation system," in *Proc. 4th Int. Joint Conf. Auto. Agents Multiagent Syst. (AAMAS)*, 2005, pp. 478–485.

[18] J. García-Nieto, E. Alba, and A. C. Olivera, "Swarm intelligence for traffic light scheduling: Application to real urban areas," *Eng. Appl. Artif. Intell.*, vol. 25, no. 2, pp. 274–283, 2012.

[19] M. Wiering, "Multi-agent reinforcement learning for traffic light control," in *Proc. 17th Int. Conf. Mach. Learn. (ICML)*, 2000, pp. 1151–1158.

[20] L. Wu, X. Xiao, D. Deng, G. Cong, A. D. Zhu, and S. Zhou, "Shortest path and distance queries on road networks: an experimental evaluation," in *Proc. 38th Int. Conf. Very Large Data Bases (VLDB)*, vol. 5. 2012, pp. 406–417.

[21] P. Li, M. Abbas, R. Pasupathy, and L. Head, "Simulation-based optimization of maximum green setting under retrospective approximation framework," *Transp. Res. Rec., J. Transp. Res. Board*, no. 2192, pp. 1–10, 2010.

[22] P. Li, P. Mirchandani, and X. Zhou, "Simulation-based traffic signal optimization to minimize fuel consumption and emission: A Lagrangian relaxation approach," in *Proc. Transp. Res. Board 94th Annu. Meeting*, 2015, pp. 2358–2374.

[23] W. Narzt *et al.*, "Self-organization in traffic networks by digital pheromones," in *Proc. IEEE 10th Int. Conf. Intell. Transp. Syst. Conf. (ITSC)*, Sep./Oct. 2007, pp. 490–495.

[24] Y. Tian, J. Song, D. Yao, and J. Hu, "Dynamic vehicle routing problem using hybrid ant system," in *Proc. IEEE 6th Int. Conf. Intell. Transp. Syst. (ITSC)*, vol. 2. Oct. 2003, pp. 970–974.

[25] B. Park, C. Messer, and T. Urbanik, II, "Enhanced genetic algorithm for signal-timing optimization of oversaturated intersections," in *Proc. Transp. Res. Board 79th Annu. Meeting*, 2000, pp. 1661–1680.

[26] N. de Lamberterie, M. Ramezani, A. Skabardonis, and N. Geroliminis, "A clustering approach for real-time control of queue spillbacks on signalized arterials," in *Proc. Transp. Res. Board 93rd Annu. Meeting*, 2014, pp. 711–726.

[27] K. Jang, H. Kim, and I. G. Jang, "Traffic signal optimization for oversaturated urban networks: Queue growth equalization," *IEEE Trans. Intell. Transp. Syst.*, vol. 16, no. 4, pp. 2121–2128, Aug. 2015.

[28] H. Yang and S. Yagar, "Traffic assignment and signal control in saturated road networks," *Transp. Res. A, Policy Pract.*, vol. 29, no. 2, pp. 125–139, 1995.

[29] P. Li, P. Mirchandani, and X. Zhou, "Solving simultaneous route guidance and traffic signal optimization problem using space-phase-time hypernetwork," *Transp. Res. B, Methodol.*, vol. 81, pp. 103–130, Nov. 2015.

[30] M. M. De Weerdt, E. H. Gerding, S. Stein, V. Robu, and N. R. Jennings, "Intention-aware routing to minimise delays at electric vehicle charging stations," in *Proc. 23rd Int. Joint Conf. Artif. Intell. (IJCAI)*, 2013, pp. 83–89.

[31] J. Li, Q. Wu, and D. Zhu, "Route guidance mechanism with centralized information control in large-scale crowd's activities," in *Proc. Int. Joint Conf. Artif. Intell. (IJCAI)*, 2009, pp. 7–11.

[32] C. P. van Hinsbergen, J. W. van Lint, and F. M. Sanders, "Short term traffic prediction models," in *Proc. 14th World Congr. Intell. Transp. Syst.*, 2007, pp. 1–18.
[33] E. I. Vlahogianni, M. G. Karlaftis, and J. C. Golias, "Short-term traffic forecasting: Where we are and where we're going," *Transp. Res. C, Emerg. Technol.*, vol. 43, pp. 3–19, Jun. 2014.
[34] S. Oh, Y.-J. Byon, K. Jang, and H. Yeo, "Short-term travel-time prediction on highway: A review of the data-driven approach," *Transp. Rev.*, vol. 35, no. 1, pp. 4–32, 2015.
[35] C. C. Chang and C. J. Lin, "LIBSVM: A library for support vector machines," *ACM Trans. Intell. Syst. Technol.*, vol. 2, no. 3, pp. 1–27, 2011.
[36] S. Kurihara, H. Tamaki, M. Numao, J. Yano, K. Kagawa, and T. Morita, "Traffic congestion forecasting based on pheromone communication model for intelligent transport systems," in *Proc. 11th Conf. Congr. Evol. Comput.*, 2009, pp. 2879–2884.
[37] W.-C. Hong, Y. Dong, F. Zheng, and C.-Y. Lai, "Forecasting urban traffic flow by SVR with continuous ACO," *Appl. Math. Model.*, vol. 35, no. 3, pp. 1282–1291, 2011.
[38] L. Song, "Improved intelligent method for traffic flow prediction based on artificial neural networks and ant colony optimization," *J. Converg. Inf. Technol.*, vol. 7, no. 8, p. 272, 2012.
[39] Z. Liang and Y. Wakahara, "A route guidance system with personalized rerouting for reducing traveling time of vehicles in urban areas," in *Proc. IEEE 17th Int. Conf. Intell. Transp. Syst. (ITSC)*, Oct. 2014, pp. 1541–1548.
[40] V. Pillac, M. Gendreau, C. Guéret, and A. L. Medaglia, "A review of dynamic vehicle routing problems," *Eur. J. Oper. Res.*, vol. 225, no. 1, pp. 1–11, 2013.
[41] S. Jiang, J. Zhang, and Y.-S. Ong, "A pheromone-based traffic management model for vehicle re-routing and traffic light control," in *Proc. 13th Int. Joint Conf. Auto. Agents Multiagent Syst. (AAMAS)*, 2014, pp. 1479–1480.
[42] B. S. Kerner, "Physics of traffic gridlock in a city," *Phys. Rev. E*, vol. 84, no. 4, p. 045102, Oct. 2011.
[43] A. Wegener, M. Piórkowski, M. Raya, H. Hellbrück, S. Fischer, and J.-P. Hubaux, "TraCI: An interface for coupling road traffic and network simulators," in *Proc. 11th Commun. Netw. Simulation Symp. (CNS)*, 2008, pp. 155–163.
[44] R. Herring, A. Hofleitner, P. Abbeel, and A. Bayen, "Estimating arterial traffic conditions using sparse probe data," in *Proc. 13th Int. IEEE Conf. Intell. Transp. Syst. (ITSC)*, Sep. 2010, pp. 929–936.
[45] Y. Wang, Y. Zheng, and Y. Xue, "Travel time estimation of a path using sparse trajectories," in *Proc. 20th ACM SIGKDD Int. Conf. Knowl. Discovery Data Mining*, 2014, pp. 25–34.
[46] Z. Cao, H. Guo, J. Zhang, D. Niyato, and U. Fastenrath, "A data-driven method for stochastic shortest path problem," in *Proc. 17th IEEE Conf. Intell. Transp. Syst. (ITSC)*, Oct. 2014, pp. 1045–1052.
[47] J. G. Wardrop, "Some theoretical aspects of road traffic research," *Proc. Inst. Civil Eng.*, vol. 1, no. 3, pp. 325–362, May 1952.
[48] Y. Zhao, S. Wang, S. Xu, X. Wang, X. Gao, and C. Qiao, "Load balance vs energy efficiency in traffic engineering: A game theoretical perspective," in *Proc. 32nd INFOCOM*, 2013, pp. 530–534.
[49] K. Tumer, Z. T. Welch, and A. Agogino, "Aligning social welfare and agent preferences to alleviate traffic congestion," in *Proc. 7th Int. Joint Conf. Auto. Agents Multiagent Syst. (AAMAS)*, 2008, pp. 655–662.

Zhiguang Cao received the B.Eng. degree in automation from Guangdong University of Technology, Guangzhou, China, and the M.Sc. degree in signal processing from Nanyang Technological University, Singapore, in 2009 and 2012, respectively. He is currently working toward the Ph.D. degree with the Future Mobility Research Laboratory, Nanyang Technological University, Singapore.

His research interests focus on the applications of artificial intelligence to transportation and traffic.

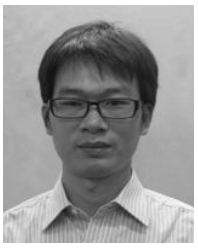

Siwei Jiang received the Ph.D. degree in computer science from Nanyang Technological University, Singapore. He is currently a Research Fellow with the Singapore Institute of Manufacturing Technology, Singapore. He has been involved in a number of industrial and in-house projects for multiobjective large-scale vehicle routing.

His research interests include areas in vehicle routing, evolutionary computation, multiobjective optimization, multiagent system, machine learning, and trust and reputation systems.

Jie Zhang received the Ph.D. degree from Cheriton School of Computer Science, University of Waterloo, Canada, in 2009. He is an Associate Professor with the School of Computer Science and Engineering, Nanyang Technological University, Singapore. During his Ph.D. study, he received the prestigious NSERC Alexander Graham Bell Canada Graduate Scholarship for top Ph.D. students across Canada.

His research has been focused on the design of effective and robust intelligent software agents, through the modeling (trustworthiness, preferences) and simulation of different agents in a wide range of environments, using AI techniques (data mining, machine learning, and probabilistic reasoning) and multi-agent technologies.

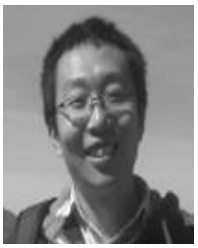

Hongliang Guo received the B.E. degree in dynamic engineering and the M.E. degree in dynamic control from Beijing Institute of Technology, China, and the Ph.D. degree in electrical and computer engineering from Stevens Institute of Technology, USA. He joined the Almende in Rotterdam, The Netherlands, as a Post-Doctoral Researcher in 2011.

In 2013, he joined NTU as a Research Fellow. In 2016 he became an Associate Professor with University of Electronics Science and Technology of China. His research interests include self-organizing systems and agent-based technologies.